HYDROLOGICAL SCIENCES JOURNAL – JOURNAL DES SCIENCES HYDROLOGIQUES, 2016
http://dx.doi.org/10.1080/02626667.2015.1133909
Special issue: *Facets of Uncertainty*

Assessing impervious area ratios of grid-based land-use classifications on the example of an urban watershed

Tatsuya Koga[a], Akira Kawamura[b], Hideo Amaguchi[b] and Hiroto Tanouchi[b]

[a]CTI Engineering Co, Ltd, Chuo-ku, Tokyo, Japan; [b]Department of Civil and Environmental Engineering, Tokyo Metropolitan University, Hachioji, Tokyo, Japan

ABSTRACT

When applying a distributed hydrological model in urban watersheds, grid-based land-use classification data with 10 m resolution are typically used in Japan. For urban hydrological models, the estimation of the impervious area ratio (IAR) of each land-use classification is a crucial factor for accurate runoff analysis. In order to assess the IAR accurately, we created a set of vector-based "urban landscape GIS delineation" data for a typical urban watershed in Tokyo. By superimposing the vector-based delineation map on the grid-based map, the IAR of each grid-based land-use classification was estimated, after calculating the IARs of all grid cells in the entire urban watershed. As a result, we were able to calculate the frequency distribution of IAR for each land-use classification, as well as the spatial distribution of IARs for the urban watershed. It is evident from the results that the reference values of IAR for the land-use classifications were estimated very roughly and inherited errors of between about 7% and 70%, which corresponds to more than 100 mm increase of direct runoff for the 1500 mm annual average precipitation.

ARTICLE HISTORY
Received 28 November 2014
Accepted 9 December 2015

EDITOR
D. Koutsoyiannis

GUEST EDITOR
E. Volpi

KEYWORDS
impervious area ratio; grid-based hydrological model; land-use classification; urban landscape GIS delineation; urban watershed; 10 m resolution

1 Introduction

1.1 Background

Watershed hydrological models are classified as distributed or lumped depending on the different schematization of the processes (Singh 1995). Distributed models take explicit account of the spatial variability of processes, inputs, boundary conditions and watershed characteristics. In most distributed models, raster-based approaches have been developed (e.g. SHE: Abbott *et al.* 1986, GSSHA: Downer and Ogden 2004, PCRaster: Karssenberg *et al.* 2010). The advantages of grid-based distributed models are their simple model structure and their use of watershed information that is generally readily available. Another advantage is the spatially explicit results that are available on each grid cell. Because of these advantages, grid-based distributed models are widely used, not only for rural but also for urban watersheds. However, various land-use classifications that inherit different impermeable properties are mixed even in one grid cell, especially in an urban watershed. Therefore, it is difficult to accurately grasp the permeable characteristics of each grid cell.

Direct runoff calculated by a hydrological model is usually based on the permeability of the surface, considering initial loss and final infiltration capacity (Ando *et al.* 1986, Toyokuni and Watanabe 1986). At an impervious surface, the only rainfall loss is the initial loss, and at a pervious surface, rainfall exceeding the final infiltration capacity contributes to direct runoff. Van de Ven *et al.* (1992) reviewed the initial loss parameters of impervious and pervious surfaces. Ando *et al.* (1986) measured final infiltration capacities of different land uses in urban watersheds. The contributing direct runoff from pervious areas is significantly smaller than that from impervious areas. Especially in urban applications, direct runoff in each grid cell is usually calculated based on estimated fractions of impervious area or estimated runoff coefficients in different land-use categories (e.g. Choi and Ball 2002, Niehoff *et al.* 2002, Park *et al.* 2008).

An increased impervious surface area is the primary agent responsible for the hydrologic changes associated with the urbanization process. Accuracy in the evaluation of impervious surface type and extent has significant implications for prediction of impervious surface impacts on watershed hydrology. The most general measure of imperviousness is total impervious surface area (TIA), usually expressed as a proportion or percentage of total area (Shuster *et al.* 2005). The hydraulically connected portion of TIA is known as directly connected impervious area (DCIA). Several studies have attempted to estimate DCIA using a high-resolution digital elevation model (DEM), multi-spectral satellite image and digital stormwater drainage pipe network database (Han and Burian 2009, Kunapo *et al.* 2009). The extent, connectedness, location and geometry of an impervious area are also likely to be important co-factors of imperviousness impacts (Shuster *et al.* 2005). However, due to lack of availability of required data and estimation difficulties, TIA is also widely accepted as an indicator of urbanization for hydrological modelling and

CONTACT Tatsuya Koga t-koga@ctie.co.jp CTI Engineering Co; Ltd, 3-21-1, Nihonbashihamacho, Chuo-ku, Tokyo 103-8430, Japan

hydro-ecological studies (Chowdhury *et al.* 2010). Regarding the impacts of impervious surface on watershed hydrology, the reader is referred to Shuster *et al.* (2005), who comprehensively reviewed the previous studies and presented a literature review on the quantitative relationships between the extent and type of impervious area and the hydrologic characteristics such as shorter concentration times and higher runoff peaks.

Estimation of impervious surface area is a pre-requisite to compute TIA. Therefore, an accurate estimation of watershed imperviousness is of current interest to urban hydrology researchers (Chabaeva *et al.* 2009, Chowdhury *et al.* 2010). There is a need for a consistent and replicable technique to easily and quickly calculate watershed imperviousness from readily available and cost-effective remote sensing information and other geo-spatial data that achieves an acceptable level of accuracy (Civco *et al.* 2006). A number of studies have been published during the past few decades that try to identify the impervious surface areas in urban watersheds using remote sensing techniques such as satellite imagery and/or aerial photos. These studies proposed various methods (e.g. Slonecker *et al.* 2001, Thomas *et al.* 2003, Yang *et al.* 2003, Yuan *et al.* 2008, Weng 2012, Sugg *et al.* 2014). However, their methodologies need the highly accurate and precise calibration and validation surface data (i.e. the ground truthing data) of the watershed to be compared with in order to assess their estimation errors. The TIA estimates of a target urban watershed by remote sensing data generally involve a not small uncertainty (Civco *et al.* 2006, Chabaeva *et al.* 2009). Furthermore, indirect assessments of impervious surface via remote sensing data can be reasonably robust, but these generally require a ground truthing level-of-effort similar to manual methods (Yang 2002).

The classification of impervious surface in conurbations with high heterogeneity in land-use patterns poses significant challenges to the delineation and classification of impervious areas (Shuster *et al.* 2005). It is apparent that there is no universal estimate of percent impervious surface cover for any particular land use. A delineation methodology that is both widely and uniformly employed is required (Leopold 1991), and needs to be made consistent in order to promote compatibility among studies in different regions. To obtain the above-mentioned ground truthing surface data of a watershed, earlier strategies were based largely on user-guided, manual delineation (Lee and Heaney 2003, Shuster *et al.* 2005, Sugg *et al.* 2014). To quantify land-use categories, Wibben (1976) used a combination of county property maps, aerial photographs and visual inspection of recorded information. Karvonen *et al.* (1999) delineated hydrologically similar units on the basis of land use, slope, soils and vegetation. For highly urbanized areas with mixed development, Walesh (1989) derived isochrones representing equivalent travel times along sewerage to a sub-basin outlet (Shuster *et al.* 2005). Chabaeva *et al.* (2009) used photogrammetrically derived calibration and validation data from high spatial resolution digital planimetric datasets to assess the results from various techniques, including remote sensing methods, for estimating the percentage of impervious surface. The major disadvantage of manual delineation is the time and effort required to produce delineations, thus limiting application to small areas (McMahon 2007).

In contrast to current modelling approaches, which are generally based on grid data (e.g. Hsu *et al.* 2000, Ettrich *et al.* 2005, Dey and Kamioka 2007, Cuo *et al.* 2008), the recent advances in GIS technology, as well as data availability, open up new possibilities concerning urban runoff modelling. A few non-raster-based models have been developed from an urban morphology viewpoint that allow consideration of individual features in the urban environment. Sample *et al.* (2001) used GIS to facilitate urban storm water analysis by using land-use parcel boundaries (apartment, commercial, low- and medium-density residential and school). Rodriguez *et al.* (2003) proposed a vector-based watershed description based on information in so-called urban databanks, which include the categories: cadastral parcel, building, street, sewer system and river, to calculate urban unit hydrographs. Rodriguez *et al.* (2008) employed the same concept to develop an urban water budget model. Although their vector-based data were intended for lumped hydrological models, and the land-use types are simple, availability of these GIS data can significantly reduce the time and effort for land-use discrimination compared to manual delineation.

The authors of this paper also proposed and developed the TSR (Tokyo Storm Runoff) model that can simulate urban storm runoff and flood inundation with a vector-based watershed description, which exactly delineated the pervious and impervious land surface features, for a typical urban watershed in Tokyo, Japan (Amaguchi *et al.* 2010, 2012). The TSR model employs so-called "urban landscape GIS delineation" that realistically describes the complicated urban land-use features in detail (see Section 2.3). In the TSR model, GIS is used to divide the urban environment into its smallest, perfectly homogeneous elements, including sewer network systems that are hydraulically connected. One key advantage of the detailed delineation is that flow tracking is possible on an element-to-element basis (Amaguchi *et al.* 2012). Furthermore, the authors have previously evaluated the hydrologic effects of ground truthing and grid-based data by using the TSR model and a grid-based model for a small sample urban watershed with a total area of 1.2 km^2 (Amaguchi *et al.* 2010). The results showed that not only does the grid-based model overestimate the runoff rate by as much as 20% more than the TSR model, but also there are significant differences in the inundation area and depth between the two models.

1.2 Object of the study

The impervious area ratio (IAR) that is basically defined as the ratio of TIA in a single grid cell (or in a land-use category) is the most important index representing the direct runoff characteristic of grid-based hydrological models. A proper estimation of the IAR of a grid cell (or of each land-use category) is therefore crucial for accurate runoff simulation in urban systems, with their high degree of imperviousness (Leopold 1968). In fact, Amaguchi *et al.* (2010) clearly show that estimation of IAR in each grid cell has a great effect on not only the direct runoff rate but also the distribution of inundation area and depth.

In Japan, grid-based hydrological models typically utilize two kinds of readily available "digital map information data" published by the Geospatial Information Authority of Japan. One has 100 m resolution and covers the whole of Japan, and the other has 10 m resolution and only contains data for three major metropolitan regions of Japan. In these metropolitan regions, grid-based land-use classification data at 10-m resolution are generally used for urban watershed hydrological models as the only source of basic data. However, as these data were established for the purpose of city planning, the impermeable properties of the grid cells are not taken into account. Each 10-m resolution grid cell is assigned only one dominant land-use classification out of the 17 categories, such as "industrial land", "commercial land", "low-rise residential land", etc. Then, the IAR of the grid cell is set automatically according to its land-use classification. Even in a small 10 m × 10 m grid cell, however, there may exist a wide range of pervious and impervious features, especially in urban watersheds in Japan (Amaguchi *et al.* 2012). This makes it more difficult to accurately estimate the IAR of each land-use classification, l*et al*one estimate the IARs of all the grid cells in the entire watershed. At present, the IAR of each classification is s*et al*most empirically in the corresponding hydrological models with reference to the related literature (e.g. Public Works Research Institute 2000, 2002), in which some test grid cells of each land-use classification were selected in a sample watershed to estimate the IARs of the land-use classifications. So far, no papers/reports have been published on accurately estimating IARs for the land-use classifications and for all grid cells in the target urban watershed, because no reference GIS data exist for that purpose in Japan.

When using computer models of watershed hydrology, there exist four types of uncertainty: (1) natural randomness, (2) data, (3) model parameters, and (4) model structure (Melching 1995). In this study, we focused on the uncertainty of a model parameter (i.e. IAR) involved in grid-based distributed models. We think that the surest method to calculate IAR is just to superimpose ground truthing data, which delineate impervious and pervious surface area completely, on the grid-based data. In order to assess the IARs of grid-based land-use classifications in an urban watershed, we created a set of vector-based "urban landscape GIS delineation" data as ground truthing data for a sub-watershed of the Kanda River, a densely-populated typical urban watershed in Tokyo, Japan. Taking full advantage of the vector-based data that exactly delineate the pervious and impervious features into 20 land-use types in the watershed, we accurately estimated the IAR of each grid-based land-use classification with 10-m resolution for the first time, after assessing the IARs of all grid cells in the entire urban watershed by simply superimposing the vector-based delineation map on the grid-based map. The frequency distribution of IAR for each land-use classification and the spatial distribution of IARs among all the grid cells in the entire watershed were also clarified to improve our ability to assess IARs using the grid-based land-use classification data.

2 Land-use information of study area

2.1 Study area

The study area selected for assessing the IARs of grid-based land-use classifications is the Upper Kanda watershed located in the Tokyo Metropolis, Japan, as shown in Fig. 1. The Kanda River is the largest small to medium-sized river in Tokyo. It has a watershed area of 105.0 km^2, and a flow path extending to 25.5 km. The annual average precipitation and evapotranspiration of the Kanda watershed are about 1500 and 230 mm, respectively (Inter-Ministry/Agency Coordination Committee for Building Sound Water Cycle 2003). This low evapotranspiration ratio of about 15% is due to the effect of high urbanization of the watershed. The Upper Kanda watershed area covers about 11.5 km^2, and the length of the river inside it is about 9 km long. The study area has been typically urbanized and densely populated, but there are still quite a few parks and forest-lands. The IAR of the study area has not yet been investigated. Figure 2 shows an example of a typical 100 m × 100 m area of the watershed depicting the relationship between the 10 m × 10 m grid cells and individual land surface features.

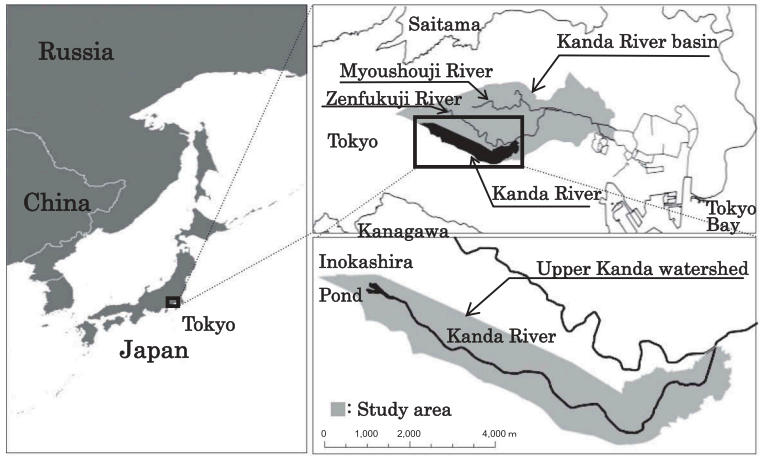

Figure 1. Location of the study area.

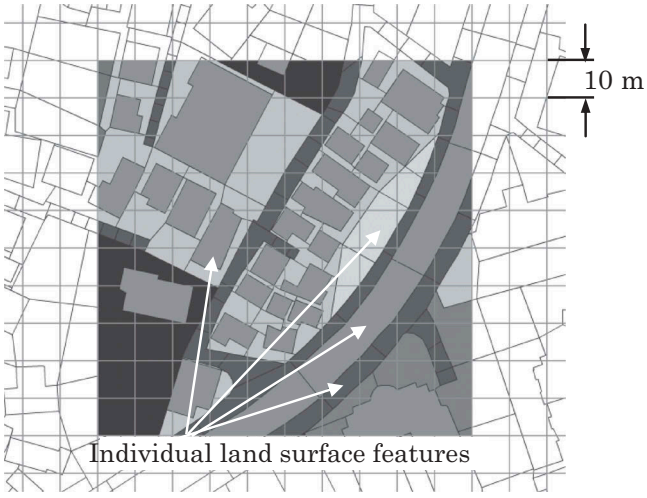

Figure 2. Relationship between 10 m × 10 m grid cells and individual land surface features.

2.2 Grid-based land-use classifications

The grid-based land-use classification data that are generally used as the basic data source for urban hydrological models are a set of land-use data with 10 m × 10 m grid cells in the plane rectangular coordinate system. These grid-based land-use classification data, which are commercially available, are established and published by the Geospatial Information Authority of Japan. Table 1 (column 2) describes the basic properties of grid-based land-use classifications. There are 17 land-use categories defined without considering the impermeable properties. Table 2 presents the statistics of the study area represented by the grid-based land-use classification. The table shows that no grids correspond to the classification numbers 2, 15, 16, 17 exist in this study area. Thus there are 13 classifications out of 17 in the study area. The total number of grids amount to more than 113 000 (Table 2, column 3). Figure 3(a) shows the spatial distribution of 13 grid-based land-use classifications, in which the 100 m × 100 m grid area is indicated enlarged. From Table 2 (columns 2–5), the "Low-rise residential land" classification is the most dominant, occupying about 51% of the study area, followed by "Road" covering 12% of the area. As a result, "Urbanized" areas occupy about 75% of the watershed, where "Urbanized" areas are usually defined to include land-use classifications "Industrial land", "Low-rise residential land", "Densely developed low-rise residential land", "Medium and high-rise residential land", "Commercial land" and "Road". It should be noted again that these grid-based land-use classifications were defined without considering their impermeable properties.

Table 1. Basic properties of the grid-based land-use classifications and the vector-based land-use types by urban landscape GIS delineation.

1	2	3
Item	Grid-based land-use classifications	Vector-based land-use types
Data format	Raster	Vector
Implementer	Geospatial Information Authority of Japan (published data)	The authors
Number of land-use categories	17	20
Impermeable property	Not considered	Considered
Shape	10 m × 10 m grid	Polygon
Data source	1/10 000 aerial photo	The vector-based basic GIS delineation data, and a 1/2500 topographic paper map

2.3 Vector-based land-use types by urban landscape GIS delineation

The urban landscape GIS delineation divides land surface in the watershed into homogeneous features exactly as seen on the surface map. These GIS data were constructed by the authors, and basic properties are shown in Table 1 (column 3). The original data sources used in the urban landscape GIS delineation are the vector-based basic GIS delineation data and a 1/2500 topographic paper map provided by the Tokyo Metropolitan Government. The basic GIS delineation data only contain the polygon data of roads, rivers and buildings. Block polygons, which are defined as the areas enclosed by road and river polygons, were further divided into individual land-use surface polygons manually according to their permeability using topographic maps, aerial photographs, and actual field survey data by the authors. As a result, the watershed was divided into a total of 20 land-use type polygons, including road, river and building polygons, as shown in Table 3 (column 2). Impervious surface types naturally include buildings, roads and paved areas etc., whereas forests, grassy areas and bare land etc. are considered pervious. The land-use types for parking lots, athletic fields, and tennis courts are categorized into two different pervious/impervious types, as shown in Table 3. The impervious types are represented by the imperviousness index $f_t = 1$, whereas pervious types are represented by $f_t = 0$, as indicated in column 3 in Table 3. Regarding the type of private premises ($t = 13$ in Table 3), buildings inside the premises are exactly delineated as "building" type, but other surfaces inside the private premises are combinations of various kinds of pervious/impervious surface features, so that in this study its imperviousness index is roughly set to $f_t = 0.5$ according to our field survey estimate. For actual urban hydrological modelling, the individual polygons such as roads, rivers, private premises, large parks, are further divided into smaller polygons, which is the smallest spatial calculation unit used in the urban runoff model (Amaguchi *et al.* 2012). Although such further divisions are not necessary for assessing the IAR of the grid-based land-use classifications, the main purpose of urban landscape GIS delineation is for urban storm runoff and flood inundation simulations with a vector-based watershed description; therefore, in this study further divisions were carried out.

Table 3 shows the statistics of the final land-use types for the Upper Kanda watershed using the urban landscape GIS delineation. The study is comprised of more than 104 000 homogeneous land surface features. This number is less than that of grid cells in Table 2. Figure 3(b) shows the spatial distribution of those land surface features into the 20 land-use types, with the same 100 m × 100 m grid area as in Fig. 3(a) enlarged. From Table 3, the two largest land-use types are

Table 2. Statistics of the study area using the grid-based land-use classification. TIA: total impervious area.

1	2	3	4	5	6	7	8	9
Grid-based land-use classifications					Urban landscape GIS delineation		Reference value	Difference
Classification c	Land-use classification	Number of grids, N_c	Area, A_c (m^2)	Area ratio, $(A_c/A)\times100$ (%)	TIA (m^2)	IAR_c (%)	IAR'_c (%)	IAR_c- IAR'_c (%)
1	Forest	1 522	152 198	1.34	40 266	26.46	0	26.46
2	Paddy field	0	0	0.00	0	–	0	–
3	Dry field & other farmlands	2 477	247 698	2.18	74 470	30.06	0	30.06
4	Arranged land	27	2 700	0.02	1700	62.97	75	−12.03
5	Vacant land	4 731	473 094	4.17	317 040	67.01	0	67.01
6	Industrial land	695	69 499	0.61	60 189	86.60	80	6.60
7	Low-rise residential land	57 445	5 744 402	50.66	4 144 170	72.14	85	−12.86
8	Densely developed low-rise residential land	2 908	290 795	2.56	227 504	78.24	90	−11.76
9	Medium and high-rise residential land	2 635	263 496	2.32	170 042	64.53	80	−15.47
10	Commercial land	7 068	706 790	6.23	569 609	80.59	95	−14.41
11	Road	13 989	1 398 859	12.34	1 107 847	79.20	100	−20.80
12	Park	9 673	967 288	8.53	273 978	28.32	20	8.32
13	Public facility	9 568	956 788	8.44	628 812	65.72	85	−19.28
14	River, Lake, etc	656	65 599	0.58	61 137	93.20	50	43.20
15	Other land use	0	0	0.00	0	–	30	–
16	Sea	0	0	0.00	0	–	–	–
17	Non investigated area	0	0	0.00	0	–	–	–
Total		N = 113 394	A = 11 339 205	100.00	7 676 763	IAR_e = 67.70	IAR'_e = 75.16	$IAR_e - IAR'_e$ = −7.46

"Private premises (except buildings)" and "Building", with about 30% of the area each, followed by "Road" (about 16%) and "Forest" (9%). These four types account for about 84% of the watershed. From the enlarged part of the study area in Fig. 3(a) and (b), it is obvious that the grid-based land-use classification is quite coarse compared to the urban landscape GIS delineation, for use in evaluating impermeable properties.

3 Method

Based on the urban landscape GIS delineation data, we calculate IAR in each grid cell. These values are then averaged over each of 13 grid-based land-use classifications and then over the whole land-use grid. In order to calculate the IAR of the entire Upper Kanda watershed (IAR_e), as well as the IAR of the grid-based land-use classification (IAR_c), first, the percentage IAR of each grid cell i (i = 1 to N; N = 113 394, the total number of grid cells in the watershed) (IAR_i, %) needs to be calculated. This is done by superimposing the vector-based delineation map on the grid-based map and IAR_i is calculated by:

$$IAR_i = \sum_{t=1}^{n_t} \frac{a_{it}}{a_i} f_t \times 100 \quad (1)$$

where n_t is the number of land-use type t from the urban landscape GIS delineation (n_t = 20, shown in Table 3); f_t is the imperviousness index of the land-use type t (shown in Table 3, column 3); a_{it} (m^2) is the area of land-use type t in the grid cell i calculated by using the urban landscape GIS delineation data; and a_i (m^2) is the area of the grid cell i (in this study, a_i = 100 m^2 for any i). The a_i is also represented using a_{it} as follows:

$$a_i = \sum_{t=1}^{n_t} a_{it} \quad (2)$$

The a_{it} is calculated first by splitting all individual land surface features of the entire watershed, created by urban landscape GIS delineation, into 10 m × 10 m grids corresponding to the grid cells by land-use classification using the Intersect function of ArcGIS software, and then by calculating the area of land-use type t in the grid cell i.

The IAR_c (%) of the grid-based land-use classification c (c = 1 to n_c; n_c = 17, the total number of grid-based land-use categories) is estimated by:

$$IAR_c = \frac{1}{N_c} \times \sum_{i=1}^{N_c} IAR_i \times 100 \quad (3)$$

where N_c is the total number of grid cells corresponding to land-use category c.

Finally, the IAR_e (%) of the entire watershed is calculated by equation (4).

$$IAR_e = \frac{1}{N} \sum_{i=1}^{N} IAR_i = \sum_{c=1}^{n_c} \frac{A_c}{A} IAR_c \quad (4)$$

where A_c (m^2) is the total area of grid-based land-use category c (shown in Table 2, column 4); A (m^2) is the total gridded area for the entire watershed. The values of A_c and A are calculated by equations (5) and (6), respectively.

$$A_c = a_i \times N_c \quad (5)$$

$$A = \sum_{c=1}^{n_c} A_c \quad (6)$$

The total number of grid cells, N, is also represented by N_c, as follows:

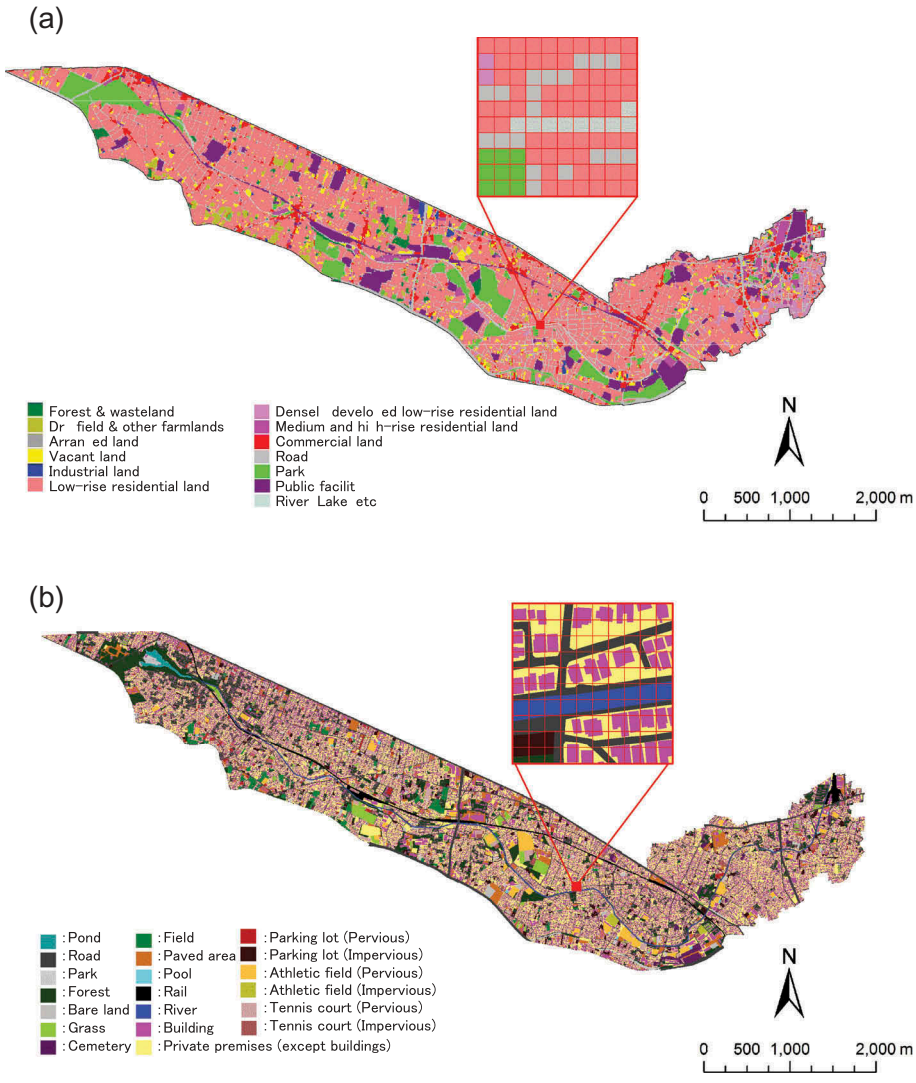

Figure 3. Spatial distribution of (a) 13 grid-based land-use classifications, and (b) individual land surface features of 20 land-use types by urban landscape GIS delineation.

$$N = \sum_{c=1}^{n_c} N_c \tag{7}$$

4 Results and discussion

Figure 4(a) shows the frequency distribution of IAR_i for all grid cells (i = 1 to N; N = 113 394) together with its mean value (i.e. IAR_e) and a reference value IAR'_e that is calculated using IAR from a previous study (Public Works Research Institute 2000). Additionally, Fig. 4(b)–(d) shows the distributions of IAR_i (i = 1 to N_c) for the grid cells with their mean values (i.e. IAR_c) and reference values IAR'_c corresponding to the three land-use classifications "Low-rise residential", "Forest", and "Road" as examples of the 13 existing classifications represented in the watershed, where IAR'_c is the IAR for each land-use classification c estimated from another urban watershed (Public Works Research Institute 2000). The rationale for the IAR'_c reference values is not clearly mentioned in the reference, but it is surmised that they are estimated empirically according to the relative degree of imperviousness in each land-use classification based on the calibration results by the grid-based model. The numbers of grid cells N_c (c = 7, 1, 11) in those classifications are indicated in the upper-right part of the figure. Table 4 shows the area, area ratio and IAR for the 20 land-use types using the urban landscape GIS delineation for the grid-based land-use classifications of Fig. 4(a)–(d). Table 2 (columns 6 and 7) shows the calculation results of TIA, IAR_c for each grid-based land-use classification and the results for the entire watershed (IAR_e). The reference values (IAR'_c and IAR'_e) often used as IAR from a previous study (Public Works Research Institute 2000), which were roughly estimated from another urban watershed, are also listed in Table 2 (column 8). Table 2 (column 9) indicates the difference between calculated and reference values (IAR_c minus IAR'_c).

From Fig. 4(a), the overall IAR of the entire watershed (IAR_e) is about 68%, and the distribution has three major peaks. The largest peak is in the IAR range of 80–85%, and there two other unexpected peaks at 100% and 0%. This

Table 3. Statistics of land-use types using the urban landscape GIS delineation.

1	2	3	4	5	6
Land-use type, t	Land-use type	Imperviousness index, f_t	Number of polygons	Area (m^2)	Area ratio (%)
1	Building	1.0	34 054	3 382 235	29.39
2	Parking lot (Pervious)	0.0	177	60 351	0.52
3	Parking lot (Impervious)	1.0	635	207 213	1.80
4	Athletic field (Pervious)	0.0	568	225 656	1.96
5	Athletic field (Impervious)	1.0	48	23 288	0.20
6	Forest	0.0	3 185	1 041 020	9.05
7	Grass	0.0	409	171 526	1.49
8	Field	0.0	483	188 587	1.64
9	Park	0.0	310	104 735	0.91
10	Cemetery	0.0	171	70 392	0.61
11	Paved area	1.0	1157	379 521	3.30
12	Rail	1.0	570	149 388	1.30
13	Private premises (except buildings)	0.5	16 765	3 432 446	29.83
14	Tennis court (Pervious)	0.0	108	54 613	0.47
15	Tennis court (Impervious)	1.0	62	30 383	0.26
16	Bare land	0.0	117	52 714	0.46
17	Pool	1.0	27	11 750	0.10
18	Road	1.0	45 104	1 785 662	15.52
19	Pond	1.0	85	36 205	0.31
20	River	1.0	307	99 704	0.87
Total		–	104 342	11 507 390	100.00

was clarified from the investigation that about 9000 completely impervious grid cells mainly came from the land-use classifications "Public facilities" and "Road", which were completely covered by impervious "Building" and "Road" land-use types, respectively. However, there were about 9000 completely pervious grid cells, which mainly correspond to "Park", "Dry field & other farmland" and "Forest" classifications. The difference between IAR_e and IAR'_e is about 7%, which suggests at most about 7% increase of direct runoff, as an error could occur when applying the reference value IAR'_e to grid-based hydrological models. In Fig. 4(b), for the "Low-rise residential land" grid cells, there is just one major peak in the same range as in Fig. 4(a), but, in contrast, there are only few grid cells with 0% or 100% IAR values. For the "Forest" grid cells in Fig. 4(c), although the reference IAR value (IAR'_c) from the Public Works Research Institute (2000) is 0%, as shown in Table 2 (column 8), there are also IARs ranging from 5% to 100%, resulting in an average IAR value (IAR_c) of 26.5%. The difference between IAR_c and IAR'_c is about 27%, suggesting a large error (at most about 27% decrease) of direct runoff involved in the "Forest" land-use classification when applying the reference value IAR'_c. Similarly, for the "Road" grid cells in Fig. 4(d), the IAR'_c is 100% (considered to be completely impervious), whereas the actual mean value (IAR_c) is about 79%. The roughly 21% difference (error) of IAR can cause more serious error than the "Forest" land-use classification, because "Road" grid cells occupy more than 12% of the watershed, compared to about 1% for "Forest" grid cells.

From Table 2 (column 9), the largest difference between IAR_c and IAR'_c occurred in the "Vacant land" classification, where the difference is about 67%. The reason is that IAR'_c (column 8) for the classification "Vacant land" is estimated as 0% (completely pervious), whereas actual "Vacant land" classification includes many impervious land-use types, such as "Buildings", "Parking lot (Impervious)", and so on. The smallest difference between IAR_c and IAR'_c is about 7% in the "Industrial land" classification (Table 2, column 9), where there is a large number of completely impervious grid cells, because many big factory buildings larger than the grid size exist, so that IAR estimation of the "Industrial land" classification is easier than the other classifications. Shuster *et al.* (2005) summarized various IAR values for several urban watersheds mainly in the USA. For example, IAR values for "Commercial land" and "Industrial land" were estimated in the ranges 80–90% and 50–90%, respectively. From Table 2 (column 7), IAR values for these classifications were estimated at 81% and 87%, respectively. The IAR value for "Commercial land" obtained in this study is the same level as the previous studies, while that for "Industrial land" is close to the upper bound of the previous studies.

In order to investigate the imperviousness characteristics of each grid-based land-use classification, we first examined the most dominant classification: "Low-rise residential land". From Table 4 (columns 7–9), almost all 19 land-use types defined by the urban landscape GIS delineation, except the "Pond" type, are mixed in the "Low-rise residential land" grid cells, although a single land-use category is assigned in the grid-based land-use classification with 10 m × 10 m resolution. In addition, actual buildings occupy only about 38% of the "Low-rise residential land" area, and there are many pervious areas such as "Private premises (except buildings)" and "Forest" in this classification. It is interesting to note that in the "Forest" classification grid cells (Table 4, columns 10–12), actual forest occupies only about 50% of the area, and impervious "Building" and "Road" areas are also involved, covering about 9% and 6%, respectively. The area ratio of "Forest" grid cells in the entire watershed is only 1.34% (Table 2, column 5), but actual forest polygons occupy 9.05% in the watershed (Table 3, column 6). In turn, in the grid cells classified as "Road" (Table 4, columns 13–15),

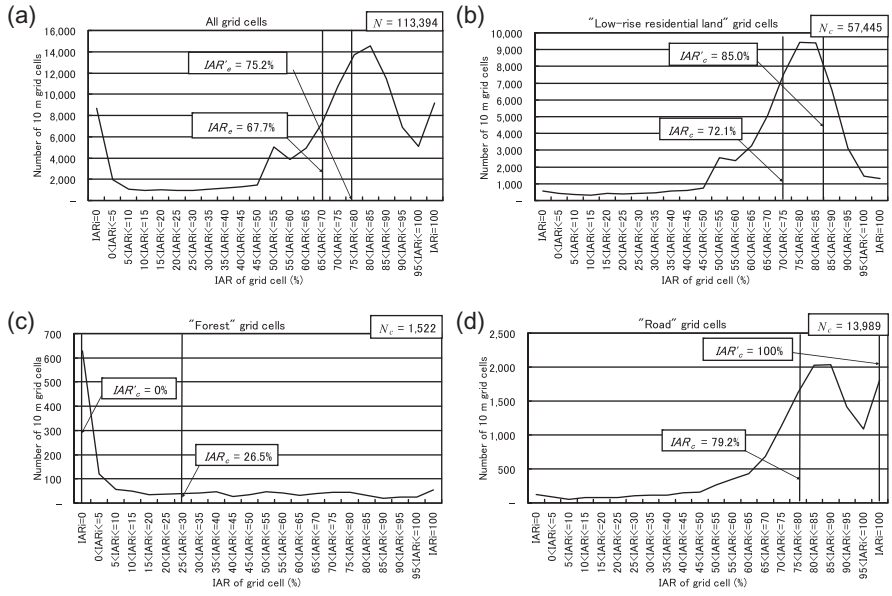

Figure 4. Frequency distribution of IAR: (a) all grid cells, (b) "Low rise residential land" grid cells, (c) "Forest" grid cells, and (d) "Road" grid cells.

actual roads occupy less than 50% of the area, and pervious areas are also significantly involved. The actual road polygons occupy 15.52% in the entire watershed (Table 3, column 6), and the area ratio of "Road" grid cells (12.34%, Table 2, column 5) is not greatly different from the actual road ratio in the watershed.

The spatial IAR distribution for all the cells calculated using the urban landscape GIS delineation, in which each individual cell has its own value, is shown in Fig. 5(a) with a 20-colour gradation. Figure 5(b) shows the spatial distribution of IAR_c of grid cells, given as the mean values of their corresponding grid-based land-use classifications (Table 2, column 7); thus the figure contains just 13 colours. Figure 5 (c) shows the spatial distribution of IAR'_c of grid cells that are assigned as reference values for the grid-based land-use classifications (Table 2, column 8), and contains only nine values (colours). Finally, Fig. 6 shows the difference between Fig. 5 (b) and (c), that is, the spatial distribution of the difference between calculated and reference values (IAR_c minus IAR'_c, as given in Table 2, column 9).

Figure 5(a) shows a wide range of IAR values, from 0% to 100%, distributed in the watershed, with both impervious (close to 100% IAR) and pervious (close to 0% IAR) grid cells being naturally dominant. When applying grid-based distributed models, setting the true IAR value for each grid cell, as shown in Fig. 5(a), is the most suitable, but it is almost impossible in actual practice unless the urban landscape GIS delineation data are available. Therefore, IAR values are generally defined based on the grid-based land-use classifications, in which one land-use classification is assigned one IAR value. Figure 5(b) shows the distribution of those IAR values (IAR_c), as given in Table 2 (column 7) for the classifications, from which the lowest IAR value is about 26% for "Forest", and the highest is about 93% for "River, Lake, etc.". These estimated values (Table 2, column 7) will be used in practice as reference IAR values for a grid-based urban distributed hydrological model. Figure 5(b) is actually the best set of IARs from a practical point of view, even though the spatial distribution of IARs mainly ranges from about 60% to 80%, eliminating 0% and 100% values. In contrast, Fig. 5(c) shows that when reference IAR values from the previous study (Table 2, column 8) are assigned to the area, then all of the IAR values are too high compared to those of Fig. 5(b). From Fig. 6, in which the grid cells with a difference between −20% and 0% are shown in yellow, the reference values are overestimated, and are dominant, occupying about 83% of all grid cells in the watershed. These grid cells comprise six land-use classifications: "Low-rise residential land", "Public facility", "Commercial land", "Densely developed", "Medium and high-rise" and "Arranged land" (Table 2, columns 5 and 9). However, the grid cells with a difference of between 0 and 20% (light blue), indicating an underestimation, occupy about 9% of all grid cells, and consist of two land-use classifications: "Park" and "Industrial land" (Table 2, columns 5 and 9). From Table 2 (column 9), the largest underestimation of 67% was in the "Vacant land" classification, while the largest overestimation of 21% was for the "Road" classification. This suggests that if the often used reference IAR values IAR'_c are applied for a grid-based urban distributed hydrological model, a significant error would be conveyed to the output results. For example, on the assumption that all the precipitation on impervious surfaces in the Upper Kanda watershed contributes to direct runoff, a 7.46% overestimation of IAR (corresponding to IAR_e minus IAR'_e indicated in Table 2, column 9) would cause an increase in direct runoff of 112 mm/year on the 1500-mm/year average annual precipitation. As a reference, Booth (2000) found that at a 10% level of effective impervious surface, runoff production increased to the extent that the post-development 2-year storm was found to yield the same amount of discharge as a 10-year pre-development storm (Shuster *et al.* 2005).

Table 4. Area, area ratio and IAR of the 20 land-use types by the urban landscape GIS delineation for the grid-based land-use classifications of Fig. 4(a)–(d).

1	2	3	4	5	6	7	8	9	10	11	12	13	14	15
Land-use type t	Land-use type	Imperviousness index, f_t	Whole grid cells			"Low-rise residential" grid cells			"Forest" grid cells			"Road" grid cells		
			Area (m^2)	Area ratio (%)	IAR (%)	Area (m^2)	Area ratio (%)	IAR (%)	Area (m^2)	Area ratio (%)	IAR (%)	Area (m^2)	Area ratio (%)	IAR (%)
1	Building	1.0	3 364 050	29.67	29.67	2 190 177	38.13	38.13	13 380	8.79	8.79	211 148	15.09	15.09
2	Parking lot	0.0	60 322	0.53	0.00	19 954	0.35	0.00	706	0.46	0.00	3 310	0.24	0.00
3	Parking lot	1.0	206 529	1.82	1.82	55 036	0.96	0.96	3 036	1.99	1.99	13 626	0.97	0.97
4	Athletic field	0.0	225 656	1.99	0.00	4 032	0.07	0.00	655	0.43	0.00	6 893	0.49	0.00
5	Athletic field	1.0	23 288	0.21	0.21	503	0.01	0.01	0	0.00	0.00	423	0.03	0.03
6	Forest	0.0	1 034 359	9.12	0.00	402 335	7.00	0.00	76 449	50.23	0.00	81 050	5.79	0.00
7	Grass	0.0	171 506	1.51	0.00	27 550	0.48	0.00	2415	1.59	0.00	8 365	0.60	0.00
8	Field	0.0	187 046	1.65	0.00	21 831	0.38	0.00	18 430	12.11	0.00	5 880	0.42	0.00
9	Park	0.0	103 925	0.92	0.00	12 985	0.23	0.00	804	0.53	0.00	11 764	0.84	0.00
10	Cemetery	0.0	70 392	0.62	0.00	1671	0.03	0.00	3	0.00	0.00	4 370	0.31	0.00
11	Paved area	1.0	378 530	3.34	3.34	103 527	1.80	1.80	4485	2.95	2.95	20 773	1.48	1.48
12	Rail	1.0	149 001	1.31	1.31	12 144	0.21	0.21	221	0.15	0.15	10 790	0.77	0.77
13	Private premises	0.5	3 403 818	30.02	15.01	2 200 893	38.31	19.16	17 352	11.40	5.70	332 299	23.76	11.88
14	Tennis court	0.0	54 612	0.48	0.00	497	0.01	0.00	470	0.31	0.00	1 358	0.10	0.00
15	Tennis court	1.0	30 383	0.27	0.27	3428	0.06	0.06	0	0.00	0.00	1 032	0.07	0.07
16	Bare land	0.0	52 714	0.46	0.00	8929	0.16	0.00	3326	2.18	0.00	1 872	0.13	0.00
17	Pool	1.0	11 750	0.10	0.10	594	0.01	0.01	0	0.00	0.00	645	0.05	0.05
18	Road	1.0	1 675 437	14.78	14.78	667 854	11.63	11.63	9517	6.25	6.25	650 189	46.48	46.48
19	Pond	1.0	36 205	0.32	0.32	0	0.00	0.00	0	0.00	0.00	0	0.00	0.00
20	River	1.0	99 681	0.88	0.88	10 461	0.18	0.18	950	0.62	0.62	33 072	2.36	2.36
Total		–	11 339 205	100.00	67.70	5 744 402	100.00	72.14	152 198	100.00	26.46	1 398 859	100.00	79.20

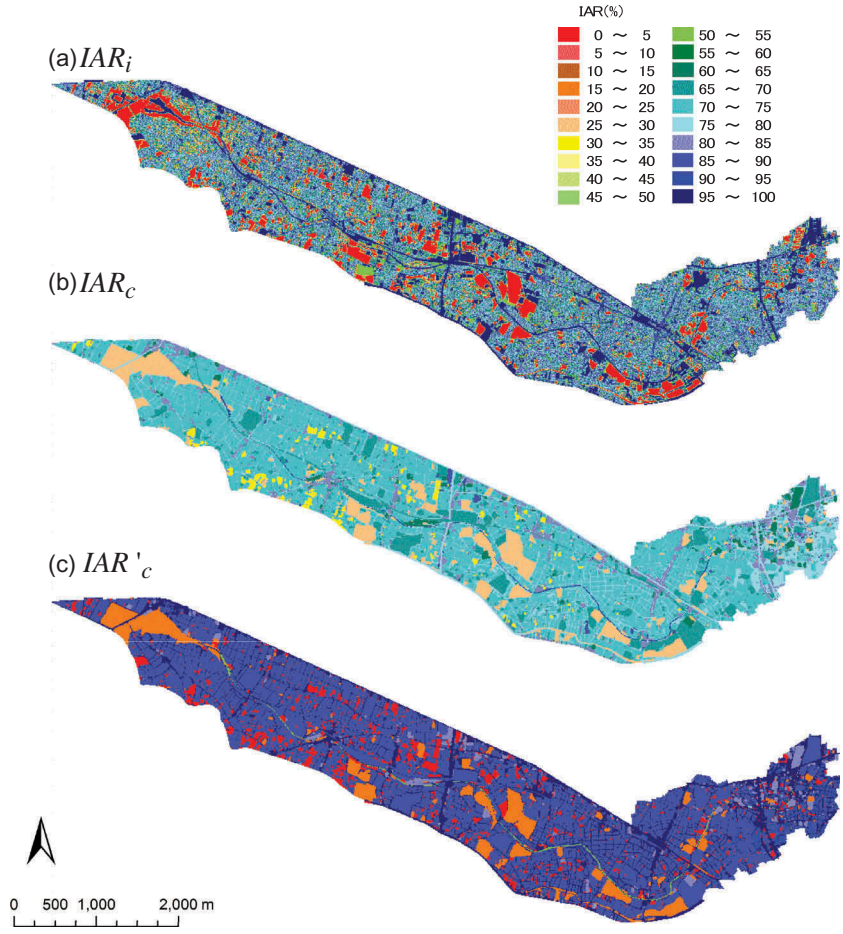

Figure 5. Spatial distribution of (a) IAR of each grid cell (IAR_i) calculated using the urban landscape GIS delineation; (b) IAR of grid cells assigned as the mean values of their corresponding grid-based land-use classifications (IAR_c); and (c) IAR of grid cells assigned as reference values (IAR'_c). .

5 Conclusion

We estimated the impervious area ratios (IARs) of grid-based land-use classifications at 10 m × 10 m resolution in an urban watershed with very high accuracy using vector-based precisely homogeneous land surface feature data implemented by the urban landscape GIS delineation technique. The IAR is a critical factor in calculating direct runoff using grid-based distributed hydrological models. The results were used to assess the error inherited in distinguishing pervious and impervious area estimates from classical grid-based land-use classification. We also analysed the impermeable characteristics of grid-based land-use classifications in the Upper Kanda watershed, a densely populated typical urban watershed, and found that a wide variety of land surface features with different impermeable properties were mixed within all land-use classifications. The analysis showed the frequency distributions of IARs for all grid cells and for the grid cells of each land-use classification. As a result, the overall IAR of the entire Upper Kanda watershed was accurately estimated to be about 68%, which was unknown until now. The actual spatial distribu-

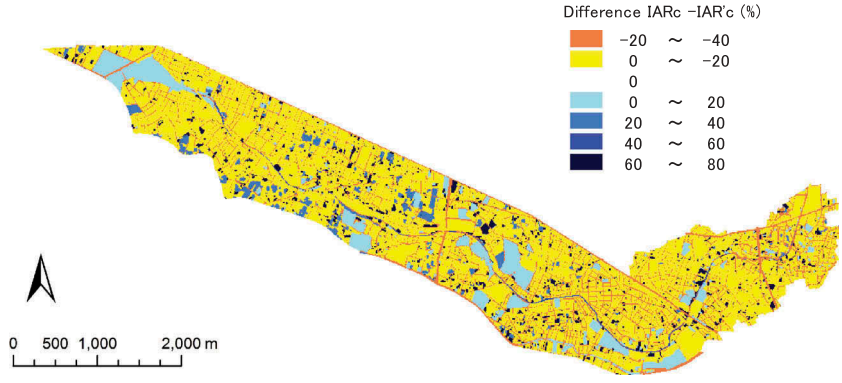

Figure 6. Difference between Fig. 5(b) and Fig. 5(c) (IAR_c minus IAR'_c).

tion of IARs in the watershed was also presented, together with a practical spatial distribution created by setting the IARs of each land-use classification as their constant mean values. The distributions were quantitatively assessed and compared with previous reference values. It is evident from the results obtained in this study that the reference values of IAR for the land-use classifications inherited about 20% overestimation and about 70% underestimation at the maximum. It is suggested that IAR should be accurately estimated for each urban watershed by creating a set of vector-based urban landscape GIS delineation data.

It is reasonable to say that the IARs obtained in this study are applicable for other highly populated urban watersheds if the impermeable properties are similar to the study area in this paper. The methodology presented here for calculating IARs would greatly contribute to improving simulation accuracy by a grid-based distributed hydrological model. In addition, the developed urban landscape GIS delineation data may be effectively used as ground truthing data to evaluate identified impervious areas obtained by remote sensing techniques. In this way, the methodology presented here has the potential to derive a guideline for correction of reference values of IARs in Japan. To this end, it is necessary to establish a vector-based landscape GIS delineation database, and to utilize the presented methodology for evaluating the IARs for other watersheds, including not only urban but also rural and test watersheds that have not applied in this study, in order to increase the number of samples of IARs. The main disadvantage of this methodology, however, is the time and effort required to create the vector-based urban landscape GIS delineation data, in which individual land-use surface polygons have to be manually delineated according to their permeability. The authors have already attempted to develop an automated delineation algorithm (Tanouchi *et al*. 2013, 2014). The ground truthing data created by such an automated algorithm would greatly contribute to accurate evaluation of IARs used in grid-based hydrological models.

Acknowledgements

We are very grateful to the reviewers for their dedicated corrections and suggestions, which have greatly contributed to marked improvements in the content of our research project.

Disclosure statement

No potential conflict of interest was reported by the authors.

Funding

This study was carried out as part of the research project "Solutions for water-related problems in Asian Metropolitan areas" supported by the Tokyo Metropolitan Government, Japan (represented by Dr Akira Kawamura).

References

Abbott, M.B., *et al*., 1986. An introduction to the European hydrological system – Système hydrologique Européen, "SHE", 1: history and philosophy of a physically-based, distributed modelling system. *Journal of Hydrology*, 87, 45–59. doi:10.1016/0022-1694(86)90114-9

Amaguchi, H., *et al*., 2012. Development and testing of a distributed urban storm runoff event model with a vector-based catchment delineation. *Journal of Hydrology*, 420-421, 205–215. doi:10.1016/j.jhydrol.2011.12.003

Amaguchi, H., *et al*., 2010. Effect of surface representation of distributed urban flood runoff models on flood hydrograph. *Annual Journal of Hydraulic Engineering*, 54, 493–498. (in Japanese with English abstract).

Ando, Y., *et al*., 1986. Urban flood modeling considering infiltration various land uses. *In*: Č. Maksimović and M. Radojković, eds. *Urban drainage modelling*. Oxford, UK: Pergamon Press.

Booth, D.B., 2000. *Forest cover, impervious surface area, and the mitigation of urbanization impacts in King county, Washington*. Department of Civil and Environmental Engineering, University of Washington.

Chabaeva, A., Civco, D., and Hurd, J., 2009. Assessment of impervious surface estimation techniques. *Journal of Hydrolic Engineering*, 14 (4), 377–387. doi:10.1061/(ASCE)1084-0699(2009)14:4(377)

Choi, K.-S. and Ball, J.E., 2002. Parameter estimation for urban runoff modelling. *Urban Water*, 4 (1), 31–41. doi:10.1016/S1462-0758(01)00072-3

Chowdhury, R., *et al*., 2010. A comparison of different methods of impervious area estimation. *In*: D.K. Begbie and S.L. Wakem, eds. *Proceedings of a science forum and stakeholder engagement: building linkages, collaboration and science quality*. Brisbane, Australia: Urban Water Security Research Alliance, 62–64.

Civco, D., Chabaeva, A., and Hurd, J., 2006. A comparison of approaches to impervious surface characterization. *IEEE Xplore* [online]. Available from: http://ieeexplore.ieee.org/xpl/articleDetails.jsp?arnumber=4241508 [Accessed 1 May 2015].

Cuo, L., *et al*., 2008. Hydrologic prediction for urban watersheds with the distributed hydrology–soil–vegetation model. *Hydrological Processes*, 22 (21), 4205–4213. doi:10.1002/hyp.v22:21

Dey, A.K. and Kamioka, S., 2007. An integrated modeling approach to predict flooding on urban basin. *Water Science & Technology*, 55 (4), 19–29. doi:10.2166/wst.2007.091

Downer, C.W. and Ogden, F.L., 2004. GSSHA: model to simulate diverse stream flow producing processes. *Journal of Hydrologic Engineering*, 9 (3), 161–174. doi:10.1061/(ASCE)1084-0699(2004)9:3(161)

Ettrich, N., *et al*., 2005. Surface models for coupled modelling of runoff and sewer flow in urban areas. *Water Science & Technology*, 52, 25–33.

Han, W.S. and Burian, S.J., 2009. Determining effective impervious area for urban hydrologic modeling. *Journal of Hydrologic Engineering*, 14 (2), 111–120. doi:10.1061/(ASCE)1084-0699(2009)14:2(111)

Hsu, M.H., Chen, S.H., and Chang, T.J., 2000. Inundation simulation for urban drainage basin with storm sewer system. *Journal of Hydrology*, 234 (1–2), 21–37. doi:10.1016/S0022-1694(00)00237-7

Inter-Ministry/Agency Coordination Committee for Building Sound Water Cycle, 2003. *Report of rehabilitation of the water cycle at the basin of the Kanda river*. Japan: Ministry of Land, Infrastructure, Transport and Tourism, 5–6 (in Japanese).

Karssenberg, D., *et al*., 2010. A software framework for construction of process-based stochastic spatio-temporal models and data assimilation. *Environmental Modelling & Software*, 25, 489–502. doi:10.1016/j.envsoft.2009.10.004

Karvonen, T., *et al*., 1999. A hydrological model for predicting runoff from different land use areas. *Journal of Hydrology*, 217, 253–265. doi:10.1016/S0022-1694(98)00280-7

Kunapo, J., Chandra, S., and Peterson, J., 2009. Drainage network modelling for water sensitive urban design. *Transactions in GIS*, 13 (2), 167–178. doi:10.1111/tgis.2009.13.issue-2

Lee, J.G. and Heaney, J.P., 2003. Estimation of urban imperviousness and its impacts on storm water systems. *Journal of Water Resources Planning and Management*, 129 (5), 419–426. doi:10.1061/(ASCE)0733-9496(2003)129:5(419)

Leopold, L.B., 1968. Hydrology for urban land planning. *US Geological Survey Circular*, 554, 1–18.

Leopold, L.B., 1991. Lag times for small drainage basins. *Catena*, 18 (2), 157–171. doi:10.1016/0341-8162(91)90014-O

McMahon, G., 2007. Consequences of land-cover misclassification in models of impervious surface. *Photogrammetric Engineering &*

Remote Sensing, 73 (12), 1343–1353. doi:10.14358/PERS.73.12.1343

Melching, C.S., 1995. Reliability estimation. In: Singh, V.P., ed. *Computer models of watershed hydrology*. Littleton, CO: Water Resources Publications, 69–118.

Niehoff, D., Fritsch, U., and Bronstert, A., 2002. Land-use impacts on storm-runoff generation: scenarios of land-use change and simulation of hydrological response in a meso-scale catchment in SW-Germany. *Journal of Hydrology*, 267, 80–93. doi:10.1016/S0022-1694(02)00142-7

Park, S.Y., *et al*., 2008. Effect of the aggregation level of surface runoff fields and sewer network for a SWMM simulation. *Desalination*, 226, 328–337. doi:10.1016/j.desal.2007.02.115

Public Works Research Institute, 2000. Development of physically-based model for water and heat cycles in urban watershed. *Technical Note of PWRI*, *3713*, 51 (in Japanese).

Public Works Research Institute, 2002. Handbook of WEP model (trial edition), 31 (in Japanese).

Rodriguez, F., Andrieu, H., and Creutin, J.-D., 2003. Surface runoff in urban catchments: morphological identification of unit hydrographs from urban databanks. *Journal of Hydrology*, 283 (1–4), 146–168. doi:10.1016/S0022-1694(03)00246-4

Rodriguez, F., Andrieu, H., and Morena, F., 2008. A distributed hydrological model for urbanized areas – model development and application to case studies. *Journal of Hydrology*, 351 (3–4), 268–287. doi:10.1016/j.jhydrol.2007.12.007

Sample, D.J., *et al*., 2001. Geographic information systems, decision support systems, and urban storm-water management. *Journal of Water Resources Planning and Management*, 127 (3), 155–161. doi:10.1061/(ASCE)0733-9496(2001)127:3(155)

Shuster, W.D., *et al*., 2005. Impacts of impervious surface on watershed hydrology: A review. *Urban Water Journal*, 2 (4), 263–275. doi:10.1080/15730620500386529

Singh, V.P., 1995. Watershed modeling. *In*: V.P. Singh, Ed. *Computer models of watershed hydrology*. Chapter 1. Littleton, CO: Water Resources Publications.

Slonecker, E.T., Jennings, D.B., and Garofalo, D., 2001. Remote sensing of impervious surfaces: A review. *Remote Sensing Reviews*, 20 (3), 227–255. doi:10.1080/02757250109532436

Sugg, Z.P., *et al*., 2014. Mapping impervious surfaces using object-oriented classification in a semiarid urban region. *Photogrammetric Engineering & Remote Sensing*, 80 (4), 343–352. doi:10.14358/PERS.80.4.343

Tanouchi, H., *et al*., 2013. Development of an automated construction algorithm of advanced delineation GIS data using 1:2500 topological map. *Journal of Japan Society of Civil Engineers, Series B1 (Hydraulic Engineering)*, 69 (4), I_523-I_528. (in Japanese with English abstract). doi:10.2208/jscejhe.69.I_523

Tanouchi, H., *et al*., 2014. Study on an automated construction method of minute road segments aiming at urban storm runoff analysis. *Theory and Applications of GIS*, 22 (2), 25–34. (in Japanese with English abstract)

Thomas, N., Hendrix, C., and Congalton, R.G., 2003. A comparison of urban mapping methods using high-resolution digital imagery. *Photogrammetric Engineering & Remote Sensing*, 69 (9), 963–972. doi:10.14358/PERS.69.9.963

Toyokuni, E. and Watanabe, M., 1986. Stormwater runoff simulations for research basin in Matsuyama City. *In*: Č. Maksimović and M. Radojković, eds. *Urban drainage modelling*. Oxford, UK: Pergamon Press.

Van de Ven, F.M.H., Nelen, A.J.M., and Geldof, G.D., 1992. Urban drainage. *In*: P. Smart and J. Herbertson, eds. *Drainage design*. Chapter 5. New York, NY: Blackie.

Walesh, S.G., 1989. *Urban surface water management*. New York, NY: Wiley-Interscience.

Weng, Q., 2012. Remote sensing of impervious surfaces in the urban areas: requirements, methods, and trends. *Remote Sensing of Environment*, 117, 34–49. doi:10.1016/j.rse.2011.02.030

Wibben, H.C., 1976. Effects of urbanization on flood characteristics in Nashville-Davidson County, Tennessee. *US Geological Survey, Water Resources Investigation Report 76-121*.

Yang, L., *et al*., 2003. Urban land-cover change detection through sub-pixel imperviousness mapping using remotely sensed data. *Photogrammetric Engineering & Remote Sensing*, 69 (9), 1003–1010. doi:10.14358/PERS.69.9.1003

Yang, X., 2002. Satellite monitoring of urban spatial growth in the Atlanta metropolitan area. *Photogramm Engineering & Remote Sensing*, 68 (7), 725–734.

Yuan, F., Wu, C., and Bauer, M.E., 2008. Comparison of spectral analysis techniques for impervious surface estimation using Landsat imagery. *Photogrammetric Engineering & Remote Sensing*, 74 (8), 1045–1055. doi:10.14358/PERS.74.8.1045